and $SnBr^+$. The relative percentage of Sn^+ is very small, which is in accord with the XPS findings that little photoreduction is occurring and also suggests that $SnBr^+$ is not further fragmenting to Sn^+ and Br^+ to any appreciable extent. Taking these factors into consideration, we propose in Scheme I various major and minor pathways for the mechanisms for photodegradation of $SnBr_2$.

Several hydrates of $SnBr_2$ have been reported.[14-16] The presence of considerable amounts of water and hydroxyl groups as shown by our RGA data suggest that the surface of our $SnBr_2$ materials is hydrated. This may account for the appearance of water and hydroxyl groups during photolysis.

Conclusions

The data presented here concern the photodegradation of $SnBr_2$. Commercial $SnBr_2$ is highly contaminated with both organic and chloride impurities. Photoreduction of $SnBr_2$ to the metallic state is enhanced when significant amounts of chloride impurity ions are present on the surface. In future studies it may be possible to dope surfaces of various semiconductors with impurity ions in order to carry out the photoreduction of semiconductors. In most experiments concerning the photolysis of $SnBr_2$ we have primarily observed photofragmentation of $SnBr_2$ and to a smaller extent have observed reduction to metallic tin. The combination of XPS, RGA, PGA, and TGA experiments allows a qualitative understanding of the processes occurring on the surface of a solid during photolysis as well as information concerning evolved gaseous species. This type of information may be of importance in the design of new material to be used as catalysts, semiconductors, or as photographic materials. The photogravimetric method described here is useful for studies of the photostability of solids.

Acknowledgment. We thank the Office of Basic Energy Sciences, Division of Chemical Sciences, Department of Energy for support of this research as well as the State of Connecticut Department of Higher Education. We thank Dr. Theo Fleisch for helpful discussions.

Registry No. Br_2Sn, 10031-24-0; Sn, 7440-31-5; SnBr, 15193-66-5; Br, 10097-32-2; SnO, 21651-19-4; HBr, 10035-10-6; H_2O, 7732-18-5.

(14) Andersson, J. *Acta Chem. Scand.* **1972**, *26*, 3813.
(15) Andersson, J. *Acta Chem. Scand.* **1972**, *26*, 2543.
(16) Andersson, J. *Acta Chem. Scand.* **1972**, *26*, 1730.

Structural Transformation of Non-Oxide Chalcogenide Glasses. The Short-Range Order of Li_2S–P_2S_5 Glasses Studied by Quantitative ^{31}P and $^{6,7}Li$ High-Resolution Solid-State NMR

Hellmut Eckert,* Zhengming Zhang, and John H. Kennedy*

Department of Chemistry, University of California, Santa Barbara, Santa Barbara, California 93106

Received November 20, 1989

The local structure of crystalline and glassy compositions in the $(Li_2S)_x(P_2S_5)_{1-x}$ system is investigated by solid-state high-resolution ^{31}P, ^6Li, and ^7Li MAS NMR. Four stable crystalline pseudobinary compounds, $LiPS_3$, $Li_4P_2S_6$, Li_3PS_4, and Li_7PS_6, are identified. The ^{31}P NMR spectra obtained on amorphous samples within the region of glass formation ($0.4 \leq x \leq 0.7$) show successive formation of sulfide analogues of metaphosphate ($Q^{(2)}$), pyrophosphate ($Q^{(1)}$), and orthophosphate ($Q^{(0)}$) species with increasing concentration of lithium sulfide. The NMR studies show unusually large chemical shift changes upon the crystallization of the glasses. For $x = 0.5$ this is believed to be due to a different type of interlinking of the $Q^{(2)}$ units. For $x = 0.67$, the $P_2S_7^{4-}$ units, which are present in the glassy phase, are quantitatively destroyed upon crystallization, leading to the formation of a $P_2S_6^{4-}$ species containing a phosphorus–phosphorus bond. The NMR results illustrate the role of the glassy state in trapping metastable local environments that have no analogues in crystalline compounds.

Introduction

The discovery of very high lithium ionic conductivity in a new class of sulfide-based glasses has been one of the most significant developments in the field of solid electrolytes in the past few years.[1-13] These glasses form by rapid quenching of melts containing Li_2S, LiI, and stoichiometric group III–V sulfides, such as B_2S_3, SiS_2, and P_2S_5. Considerable experimental work has been undertaken to maximize conductivity and chemical stability of these compounds. It has been more recently that driven by the search for structural guidelines to optimize materials properties, the microstructure of these glasses has moved into the focus of attention.[14-18]

According to most recent spectroscopic studies, chalcogenide glasses can have very unusual structures, displaying

* Authors to whom correspondence should be addressed.

(1) Malugani, J. P.; Robert, G. *Solid State* Ionics **1980**, *1*, 519.
(2) Robert, G.; Malugani, J. P.; Saida, A. *Solid State Ionics* **1981**, *3/4*, 311.
(3) Malugani, J. P.; Fahys, B.; Mercier, R.; Robert, G.; Duchange, J. P.; Baudry, S.; Broussely, M.; Gabano, J. P. *Solid State Ionics* **1983**, *9/10*, 659.
(4) Mercier, E.; Malugani, J. P.; Fahys, B.; Robert, G. *Solid State Ionics* **1981**, *5*, 663.
(5) Duchange, J. P.; Malugani, J. P.; Fahys, B.; Robert, G. *Prog. Batteries Sol. Cells* **1981**, *4*, 46.
(6) Ribes, M.; Barrau, B.; Souquet, J. L. *J. Noncryst. Solids* **1980**, *38/39*, 271.
(7) Wada, H.; Menetrier, M.; Levasseur, A.; Hagenmuller, P. *Mater. Res. Bull.* **1983**, *18*, 189.
(8) Pradel, A.; Ribes, M. *Solid State Ionics* **1986**, *18/19*, 351.
(9) Kennedy, J.; Yang, Y. *J. Solid State Chem.* **1987**, *69*, 252.

0897-4756/90/2802-0273$02.50/0

a large degree of intermediate-range order and including edge-shared coordination polyhedra, which are not found in oxidic glasses.[19-22] However, the identification and quantitative determination of specific structural features have often remained controversial, since most of the spectroscopic techniques used are not inherently quantitative and tend to emphasize ordered environments. Currently, there is a definite need for new experimental probes that can test the existing structural hypotheses in a more stringent manner than presently possible. Solid-state NMR is an element-selective, inherently quantitative method ideally suited for this objective.[23-25] For instance, in silicate glasses, ^{29}Si NMR chemical shifts can discern the various SiO_4 coordination polyhedra $Q^{(n)}$, which differ in the number n of Si–O–Si bridges per Si atom.[26-30] In a similar fashion, ^{31}P MAS NMR has provided identification of sites in phosphate glasses and corresponding crystalline phases.[31-39] Unique chemical shift ranges have been assigned to orthophosphate (PO_4^{3-} monomers, $Q^{(0)}$ species), pyrophosphate ($P_2O_7^{4-}$ dimers, $Q^{(1)}$ species), and metaphosphate units (PO_3^- chains ($Q^{(2)}$) species).[38,39] The compositional dependences of their occurrences are in quantitative agreement with the continuous network modification model, in which one oxide ion transforms one P–O–P bridge into two P atoms containing nonbridging oxygen atoms.[40]

It would be of interest to explore (a) whether similar structural principles are operative in the stoichiometrically analogous sulfide systems and (b) whether ^{31}P NMR can provide analogous structural information. So far, however, in spite of the importance of non-oxide chalcogenide glasses, NMR applications to such systems have been relatively scarce.[41-49] In the present contribution, we report the first systematic solid-state NMR study of the system Li_2S–P_2S_5. We will discuss the structure of these glasses on the basis of multinuclear (^6Li, ^7Li, and ^{31}P) MAS NMR results on glassy and crystallized samples. On the basis of the compositional dependence of the solid-state NMR spectra, we will deduce the stoichiometries of the crystalline compounds, interpret the spectral features in relationship to the published single-crystal X-ray data, and then use this information to discuss the network structure of the glassy materials.

Table I. Synthetic Conditions of the Samples Studied and Identified Phases (from X-ray Powder Diffraction and Solid-State NMR) in the System $(Li_2S)_x(P_2S_5)_{1-x}$[a]

x	experimental conditions	identified phases
0.33	melt–quench (700 °C), then annealed at 225 °C	28% $(PS_{2.5-x})$, 72% $LiPS_3$
0.40[b]	melt–quench	phase-sep glass; T_g = 162, 213 °C
0.40	melt–quench (700 °C), then annealed at 250 °C	20% $(PS_{2.5-x})$; 80% $LiPS_3$
0.50[b]	melt–quench (700 °C)	glass; T_g = 177.4 °C
0.50	melt–quench (800 °C), then annealed at 275 °C	94% $LiPS_3$, 6% Li_2PS_3
0.60[b]	melt–quench (800 °C)	glass; T_g = 196 °C
0.60	melt–quench (800 °C), then annealed at 300 °C	6% $(PS_{2.5-x})$, 94% Li_2PS_3
0.66[b]	melt–quench (800 °C)	glass; T_g = 217 °C
0.66	melt–quench (800 °C), then annealed at 325 °C	100% Li_2PS_3
0.66	melt–quench (800 °C), then annealed at 275 °C	100% Li_2PS_3
0.70[b]	melt–quench	glass; T_g = 213 °C
0.70	melt–quench (800 °C), then annealed at 350 °C	73% Li_2PS_3, 10% Li_3PS_4, 17% Li_7PS_6
0.75	melt–quench (800 °C),	phase-sep glass
0.75	melt–quench (800 °C), then annealed at 375 °C	94% Li_3PS_4
0.75	solid-state reaction, 600 °C, 1 week	70% Li_3PS_4, 30% Li_7PS_6
0.80	melt at 900 °C, decrease temperature by 100 °C/h	70% Li_3PS_4, 30% Li_7PS_6
0.80	solid-state reaction, 600 °C, 1 week	75% Li_3PS_4, 12% Li_7PS_6, 13% other, $+Li_2S$
0.875	melt at 900 °C, decrease temperature by 100 °C/h	41% Li_3PS_4, 59% Li_7PS_6, $+Li_2S$
0.875	solid-state reaction, 600 °C, 1 week	15% Li_3PS_4, 85% Li_7PS_6, $+Li_2S$

[a] Percentages are based on integration of the ^{31}P signals. [b] X-ray amorphous.

Experimental Section

Sample Preparation and Characterization. Tables I and II give an overview of the samples investigated, their preparative conditions, glass-transition temperatures, and NMR parameters.

(10) Kennedy, J. H.; Yang, Y. *J. Electrochem. Soc.* **1986**, *133*, 2437.
(11) Sahami, S. Shea, S. W.; Kennedy, J. H. *J. Electrochem. Soc.* **1985**, *132*, 985.
(12) Kennedy, J. H.; Sahami, S.; Shea, S. W.; Zhang, Z. *Solid State Ionics* **1986**, *18/19*, 368.
(13) Kennedy, J. H.; Zhang, Z.; Eckert, H. *J. Noncryst. Solids*, in press.
(14) Dembovskii, S. A.; Chechetkina, E. A. *J. Noncryst. Solids* **1986**, *85*, 346.
(15) Bicerano, J.; Ovshinsky, S. R. *J. Noncryst. Solids* **1985**, *74*, 75.
(16) Boolchand, P. *Hyperfine Interact.* **1986** *27*, 3.
(17) Phillips, J. C. *J. Noncryst. Solids* **1979**, *34*, 153.
(18) Angell, C. A. *J. Noncryst. Solids* **1985**, *73*, 1.
(19) Phillips, J. C. *J. Noncryst. Solids* **1981**, *43*, 37.
(20) Tenhover, M.; Hazle, M. A.; Grasselli, R. K. *Phys. Rev. Lett.* **1983**, *51*, 404.
(21) Griffiths, J. E.; Malyi, M.; Espinosa, G. P.; Remeika, J. P. *Phys. Rev. B* **1984**, *30*, 6978.
(22) Vashishta, P.; Kalia, R. K.; Ebbsjö, I. *J. Noncryst. Solids* **1988**, *106*, 301.
(23) Muller-Warmuth, W.; Eckert, H. *Phys. Rep.* **1982**, *88*, 91.
(24) Bray, P. J. *J. Noncryst. Solids* **1985**, *73*, 19.
(25) Turner, G. L.; Kirkpatrick, R. J.; Risbud, S. H.; Oldfield, E. *Am. Ceram. Soc. Bull.* **1987**, *66*, 656.
(26) Grimmer, A. R.; Mägi, M.; Hähnert, M.; Stade, H.; Samoson, A.; Wieker, W.; Lippmaa, E. *Phys. Chem. Glasses* **1984**, *25*, 105.
(27) Dupree, R.; Holland, D.; McMillan, P. W.; Pettifer, R. F. *J. Noncryst. Solids* **1984**, *68*, 399.
(28) Murdoch, J. B.; Stebbins, J. F.; Carmichael, I. S. E. *Am. Mineral.* **1985**, *70*, 332.
(29) Kirkpatrick, R. J.; Smith, K. A.; Kinsey, R. A.; Oldfield, E. *Am. Mineral.* **1985**, *70*, 106.
(30) Schneider, E.; Stebbins, J. F.; Pines, A. *J. Noncryst. Solids* **1987**, *89*, 371.
(31) Turner, G. L.; Smith, K. A.; Kirkpatrick, R. J.; Oldfield, E. *J. Magn. Reson.* **1986**, *70*, 408.
(32) Villa, M.; Scagliotti, M.; Chiodelli, G. *J. Noncryst. Solids* **1987**, *94*, 101.
(33) Villa, M.; Chiodelli, G.; Scagliotti, M. *Solid State Ionics* **1986**, *18/19*, 382.
(34) Villa, M.; Carduner, K. R.; Chiodelli, G. *Phys. Chem. Glasses* **1987**, *28*, 131.
(35) Villa, M.; Carduner, K. R.; Chiodelli, G. *J. Solid State Chem.* **1987**, *69*, 19.
(36) Bunker, B. C.; Tallant, D. R.; Balfe, C. A.; Kirkpatrick, R. J.; Turner, G. L.; Reidmeier, M. R. *J. Am. Ceram. Soc.* **1987**, *70*, 675.
(37) Prabhakar, S.; Rao, K. J.; Rao, C. N. R. *Chem. Phys. Lett.* **1987**, *139*, 96.
(38) Duncan, T. M.; Douglass D. C. *Chem. Phys.* **1984**, *87*, 339.
(39) Griffiths, L.; Root, A.; Harris, R. K.; Packer, K. J.; Chippendale, A. M.; Tromans, F. R. *J. Chem. Soc., Dalton Trans.* **1986**, 2247.
(40) Van Wazer, J. R. *J. Am. Chem. Soc.* **1950**, *72*, 644.
(41) Hintenlang, D. E.; Bray, P. J. *J. Noncryst. Solids* **1985**, *69*, 243.
(42) Eckert, H.; Müller-Warmuth, W.; Hamann, W.; Krebs, B. *J. Noncryst. Solids* **1984**, *65*, 53.
(43) Eckert, H.; Müller-Warmuth, W. *J. Noncryst. Solids* **1985**, *70*, 199.
(44) Eckert, H.; Zhang, Z.; Kennedy, J. H. *Mater. Res. Soc. Symp. Proc.* **1989**, *135*, 259.
(45) Zhang, Z.; Kennedy, J. H.; Thompson, J.; Anderson, S.; Lathrop, D. A.; Eckert, H. *Appl. Phys.* **1989**, *A49*, 41–54.
(46) Tenhover, M.; Boyer, R. D.; Henderson, R. S.; Hammond, T. E.; Shreve, G. A. *Solid State Commun.* **1988**, *65*, 1517.
(47) Eckert, H.; Zhang, Z.; Kennedy, J. H. *J. Noncryst. Solids* **1989**, *107*, 271.
(48) Lathrop, D.; Eckert, H. *J. Am. Chem. Soc.* **1989**, *111*, 3536.
(49) Lathrop, D.; Eckert, H. *J. Noncryst. Solids* **1988**, *106*, 417.

Table II. NMR Parameters of Glassy and Crystalline Phases in the System $(Li_2S)_x$-$(P_2S_5)_{1-x}$ and of $Ag_4P_2S_7$

	^{31}P				$^{6,7}Li$	ν_{P-P}, Hz		^7Li
sample	δ_{iso},[a] ppm	δ_{11},[b] ppm	δ_{22},[b]	δ_{33},[b] ppm	δ_{iso},[c] ppm	^6Li[d]	^7Li[e]	e^2qQ/h,[f] kHz
Glasses: $(Li_2S)_x(P_2S_5)_{1-x}$								
$x = 0.40$	83.0				1.40	nd[g]	nd	nd
$x = 0.50$	83.0				1.40	30	nd	nd
$x = 0.60$	89.8				1.55	25	nd	nd
$x = 0.66$	89.8				1.66	20	nd	nd
$x = 0.70$	86.3				1.66	20	nd	nd
Crystalline Compounds								
P_2S_5[i]	49.6	−57	106	106				
	51.5	−55	94	110				
$LiPS_3$	54.9	−155	120	195	1.76	25	200	100
$Li_4P_2S_6$	109.1	*h*	*h*	*h*	1.45	35	650	<20
	108.5	*h*	*h*	*h*				
$Ag_4P_2S_7$	96.6	*h*	*h*	*h*				
Li_3PS_4	88.4	*h*	*h*	*h*	2.80	25	480	30
Li_7PS_6	86.6	52	100	108	2.08	20	70 ± 5	<10

[a] Versus 85% H_3PO_4, ±0.1 ppm. [b] Versus 85% H_3PO_4, estimated error ±5 ppm. [c] Versus solid LiCl, ±0.05 ppm. [d] Width of ^6Li MAS centerband ± 5 Hz. [e] Width of ^7Li MAS centerband ± 20 Hz unless indicated. [f] Estimated from width of spinning sideband pattern. [g] Not determined. [h] Chemical shift anisotropies too small for accurate determination by sideband analysis. [i] From ref 54.

Since the starting and resultant materials are extremely hygroscopic and air-sensitive, all preparations were carried out under a noble-gas atmosphere with H_2O and O_2 levels less than 2 ppm. $(Li_2S)_x(P_2S_5)_{1-x}$ glasses were synthesized within evacuated quartz ampules from commercial Li_2S (99.9%) and P_2S_5 (99%, distilled). While commercial P_2S_5 is known to contain a mixture of P_4S_{10}, P_4S_9, and S_8,[50,51] these components are expected to equilibrate under the reaction conditions. The samples were heated at 800–900 °C for 0.5 h and then quenched from ca. 700–800 °C in ice water. The glassy character was verified by X-ray powder diffraction (on a fully automated Scintag diffractometer). Glass transition temperatures were measured by differential scanning calorimetry, by using a Du Pont 912 analyzer with a heating rate of 10 °C/min. All samples within the compositional range $0.5 \leq x \leq 0.7$ show single transitions (followed by recrystallization exotherms), indicating the formation of homogeneous glasses. This compositional region is substantially wider than that previously reported by Mercier and co-workers.[1-3] While the quenched $x = 0.4$ composition appeared entirely amorphous according to X-ray diffraction, the solid-state NMR spectrum shows a small amount of crystalline impurity (identified by the chemical shift as $LiPS_3$; see below). Subsequent to the NMR study, all the glassy samples were recrystallized by annealing them ca. 50 °C below their melting temperatures. The same technique was used to synthesize crystalline specimens with compositions outside of the glass-forming region. Table I summarizes the reaction conditions. The products were characterized by X-ray powder diffraction and solid-state NMR. All compositions were studied in replicate. The model compound $Ag_4P_2S_7$ was prepared according to the procedure given in the literature,[52] and its identity was established by X-ray powder diffraction.

NMR Studies. Nuclear magnetic resonance studies were carried out at 121.65 MHz on a General Electric GN-300 wide-bore system, equipped with a multinuclear magic-angle spinning probe from DOTY Scientific. Samples were spun within sapphire or zirconia spinners of 7-mm o.d. at speeds between 3 and 5 kHz. To avoid hydrolysis by atmospheric moisture, the spinners were sealed with a thin layer of high-vacuum grease and spun with evaporated liquid nitrogen. For all of the nuclei studied the 90° pulse length was 7 μs. To obtain quantitatively representative spectra, the relaxation behavior was tested by progressive saturation experiments. The final recycle delays were typically 1 min for the glassy and 10 min for the crystalline samples, found sufficient to record spectra with intensity ratios undistorted by saturation effects. Chemical shifts were externally referenced to 85% H_3PO_4 (^{31}P) and a spinning sample of dry LiCl (^6Li, ^7Li), respectively. Chemical shift anisotropies were estimated from the spinning sideband intensities, by using the graphical procedure of Herzfeld and Berger.[53] These results are reported with downfield shifts positive and δ_{11} as the most upfield component. In spectra containing multiple peaks, relative peak areas were obtained by integration or fitting to Gaussian line shapes, by using the General Electric GEMCAP software.

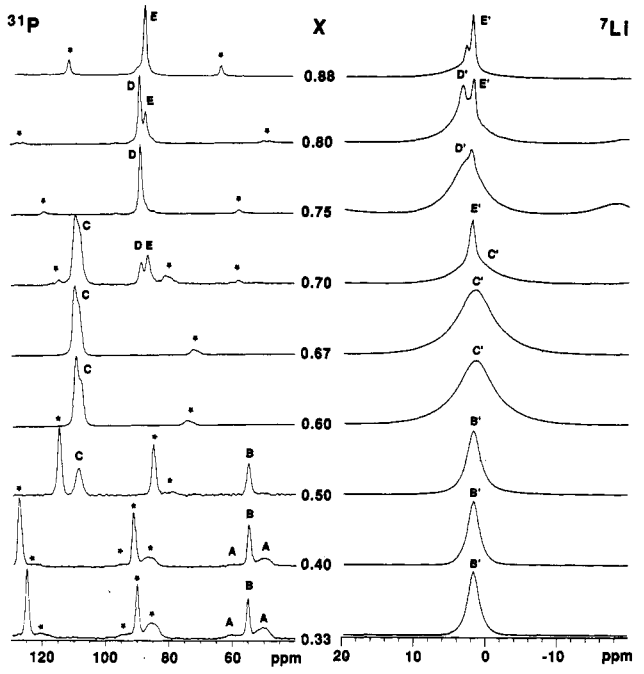

Figure 1. ^{31}P and ^7Li MAS NMR spectra in the centerband region of crystallized $(Li_2S)_x$-$(P_2S_5)_{1-x}$ samples. The respective values of x are indicated in the figure. The labels A–E and A′–E′ refer to the various crystalline compounds identified in the ^{31}P and the ^7Li MAS NMR spectra (see text). Spinning sidebands are indicated by asterisks.

Results

NMR Characterization of Crystalline Phases in the System Li_2S–P_2S_5. Figure 1 shows the ^{31}P and ^7Li MAS NMR spectra of crystallized samples with various Li_2S/P_2S_5 ratios. The compositional dependence of these spectra consistently indicates the presence of four ternary compounds (whose MAS NMR central resonances have been labeled B–E) with $x = 0.5$, 0.66, 0.75, and 0.88. (A

(50) Demarq, M. C. *Phosphorus Sulfur* **1981**, *11*, 65.
(51) Thamm, R.; Heckmann, G.; Fluck, G. *Phosphorus Sulfur* **1982**, *12*, 319.
(52) Toffoli, P.; Khodadad, P.; Rodier, N. *Acta Crystallogr.* **1977**, *B33*, 1492.
(53) Herzfeld, J.; Berger, A. E. *J. Chem. Phys.* **1980**, *73*, 6021.

solid-state NMR characterization of the compounds P_4S_{10} and P_4S_9, species A, has been previously reported.[54] The most phosphorus-rich pseudobinary compound (at $x = 0.5$, species B) has a P:Li ratio of 1:1, corresponding to a stoichiometry $LiPS_3$. To our knowledge, a compound with this stoichiometry has not been reported to date in the Li_2S–P_2S_5 system. The ^{31}P MAS NMR spectrum shows an extremely wide spinning sideband pattern, revealing a large chemical shift anisotropy (see Table II). At compositions with higher P_2S_5 contents ($x < 0.5$), the spectra can be quantitatively explained in terms of a superposition of this ternary phase with binary phosphorus sulfides (primarily P_4S_{10} and P_4S_9).

In addition to the above signal, a small amount of a new, characteristic ^{31}P resonance near 108–109 ppm, containing some discernible structure, appears at the $x = 0.5$ composition (species C). This resonance dominates the ^{31}P MAS NMR spectrum in the compositional range $0.60 \leq x \leq 0.70$. At the nominal composition $x = 0.67$ ($Li_4P_2S_7$) the chemical shift in the crystalline state differs dramatically from that of the corresponding glassy material (see below). In contrast, the value is close to the solution-state value previously observed for $Na_4P_2S_6{\cdot}6H_2O$ (the crystalline sodium analogue obtained for $x = 0.67$) in aqueous solution.[55] Replicate experiments indeed confirm that elemental sulfur is released upon crystallization of glassy $Li_4P_2S_7$, according to the reaction

$$(Li_4P_2S_7)_{glass} \rightarrow (Li_4P_2S_6)_{cryst} + \tfrac{1}{8}S_8$$

Our conclusion from NMR agrees with an earlier report by Mercier et al., who describe the structure of $Li_4P_2S_6$ single crystals grown from glass of composition $Li_4P_2S_7$ ($x = 0.67$).[56] The stoichiometry of $Li_4P_2S_6$ is analogous to that of the well-known class of hexathiohypodiphosphates.[57-59] The structure of these materials (including $Na_4P_2S_6{\cdot}6H_2O$) is based upon ethane-like staggered $P_2S_6^{4-}$ ions, containing a single phosphorus–phosphorus bond. In the present study, this P–P bond, which constitutes a more or less isolated two-spin system, was experimentally confirmed further by the observation of a $90_x°$–t –$90_y°$ solid echo (see ref 60 for a description of the methodology) over a wide range of delay times t, from 50 to 300 μs. The NMR spectra show that the above decomposition upon crystallization is complete, leaving no trace of crystalline $Li_4P_2S_7$. We note further, in agreement with ref 56, that the X-ray powder pattern assigned to $Li_4P_2S_6$ shows perfect agreement with one previously reported in the literature, which is, however, assigned to a compound with the stoichiometry $Li_8P_2S_9$.[61] On the basis of the stoichiometry of our samples (Li:P = 2:1), the observed ^{31}P and ^7Li MAS NMR spectra, and the absence of Li_2S or phosphorus sulfides in the X-ray powder patterns, we conclude that the original assignment to $Li_8P_2S_9$ in ref 61 is erroneous.

We note that the ^{31}P resonance assigned to $Li_4P_2S_6$ appears to have two components whose relative area ratio appears somewhat variable in different samples. Additional experiments at a higher field strength (11.7 T) confirm that this splitting is due to a chemical shift difference and not due to J coupling. This finding is consistent with the crystal structure of $Li_4P_2S_6$, which was solved under the assumption of random disorder of P atoms over two sites (overall occupancy factor 0.5). The NMR spectra suggest that these two sites have different chemical shifts and have somewhat variable occupancies.

Above $x = 0.7$ the ^{31}P MAS NMR spectra give rise to two additional signals at 88.4 and 86.6 ppm (species D and E), which can be assigned to Li_3PS_4 ($x = 0.75$) and Li_7PS_6 ($x = 0.88$), respectively, on the basis of the compositional dependence and the published X-ray powder pattern of Li_7PS_6.[61] The single-crystal structure of Li_3PS_4 has been previously reported[62] and is based upon isolated PS_4^{3-} ions. The X-ray diffraction powder pattern derived from this structure is in good agreement with the one observed by us. The chemical shift assigned to the PS_4^{3-} group is consistent with reference data from the early solution-state NMR study of Maier and van Wazer on the Na_2S–P_2S_5 system.[63] In agreement with the X-ray data, only a single phosphorus site is present. While the crystal structure of Li_7PS_6 is unknown, the compound is believed to be a double salt of PS_4^{3-} and S^{2-} anions, such as reported for Cu_7PS_6[64] and Ag_7PS_6.[65] The MAS NMR spectrum of Li_7PS_6 indicates the presence of a single distinct PS_4^{3-} group. The PS_4^{3-} groups present in Li_3PS_4 and Li_7PS_6 are easily distinguishable both by their isotropic chemical shifts and by the anisotropic chemical shielding information, which can be obtained by Herzfeld–Berger analysis of the slow-spinning MAS NMR spectra shown in Figure 2a. Notably, the chemical shielding tensor of Li_7PS_6 is approximately axially symmetric (see Table II), indicating that the PS_4^{3-} tetrahedron in this compound is axially distorted and maintains a 3-fold symmetry axis.

The NMR spectra and X-ray powder diffraction patterns of replicate experiments reveal that Li_7PS_6 is difficult to prepare in a pure form, i.e., without significant formation of the competing phases Li_3PS_4 and Li_2S. In addition, minority peaks at 96.5 and 84.4 ppm have been observed with reproducible intensities, possibly indicating that other phases are present. Our NMR data give, however, no evidence for the existence of $Li_8P_2S_9$ reported in ref 61.

The compositional evolution of the ^7Li MAS NMR spectra is well compatible with the findings from ^{31}P MAS NMR. As summarized in Table II, each compound is characterized by a unique chemical shift, MAS NMR line width, and ^7Li NMR spinning sideband pattern, arising from the $^3/_2 \rightarrow {}^1/_2$ and the $-{}^1/_2 \rightarrow -{}^3/_2$ transitions, which are shifted due to first-order quadrupolar perturbations. Table II includes approximate nuclear electric quadrupolar coupling constants estimated from the spectral width of the spinning sideband patterns. (For $I = {}^3/_2$, the quadrupole coupling constant is approximately equal to the entire range spanned by the powder patterns of the outer quadrupolar transitions; under the MAS condition, spinning sidebands will be observed over this range.) The $LiPS_3$ phase is distinguished by a particularly large quadrupolar coupling constant. For the remaining phases, the interaction is weak, indicating either higher symmetry of the lithium coordination or partial averaging of the interaction due to ionic diffusion at room temperature.

(54) Eckert, H.; Liang, C. S.; Stucky, G. D. *J. Phys. Chem.* **1989**, *93*, 452.
(55) Falius, H. *Z. Anorg. Allg. Chem.* **1967**, *356*, 189.
(56) Mercier, R.; Malugani, J. P.; Fahys, B.; Douglade, J.; Robert, G. *J. Solid State Chem.* **1982**, *43*, 151.
(57) Klingen, W.; Eulenberger, G.; Hahn, H. *Z. Anorg. Allg. Chem.* **1973**, 401, 97.
(58) Taylor, B. E.; Steger, J.; Wold, A. *J. Solid State Chem.* **1973**, *7*, 461.
(59) Sourisseau, C.; Forgerit, J. P.; Mathey, Y. *J. Solid State Chem.* **1983**, *49*, 134.
(60) Powles, J. G.; Strange, J. H. *Proc. Phys. Soc. London* **1963**, *82*, 6.
(61) Brice, T. *C. R. Seances Acad. Sci. Ser.* **1976**, *C283*, 581.
(62) Mercier, R.; Malugani, J. P.; Fahys, B.; Robert, G.; Douglade, J. *Acta Crystallogr.* **1982**, *B38*, 1887.
(63) Maier, L.; Van Wazer, J. R. *J. Am. Chem. Soc.* **1962**, *84*, 3054.
(64) Kuhs, F. W.; Schulte-Kellinghaus, M.; Krämer, V.; Nitsche, R. *Z. Naturforsch.* **1977**, *32b*, 1100.
(65) Toffoli, P.; Khodadad, P. *C. R. Acad. Sci. Ser.* **1978**, *286*, 349.

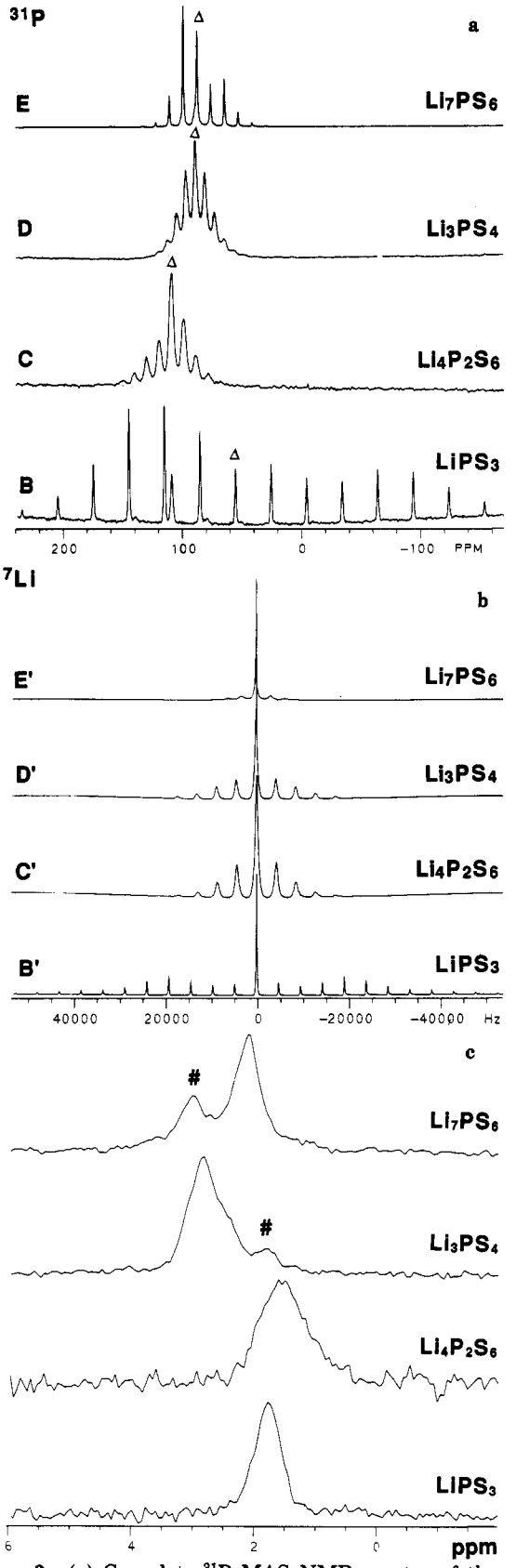

Figure 2. (a) Complete ^{31}P MAS NMR spectra of the pure crystalline compounds identified in the system Li_2S–P_2S_5. Central MAS NMR bands are indicated by the symbol Δ. (b) Complete ^{7}Li MAS NMR spectra of the pure crystalline compounds in the system Li_2S–P_2S_5. The minor peaks are spinning sidebands arising from the quadrupolar satellite transitions. (c) ^{6}Li MAS NMR spectra of the crystalline compounds in the system Li_2S–P_2S_5. The symbol # denotes minor impurity phases present in the samples. These impurities are Li_7PS_6 in the Li_3PS_4 sample and Li_2S in the Li_7PS_6 sample.

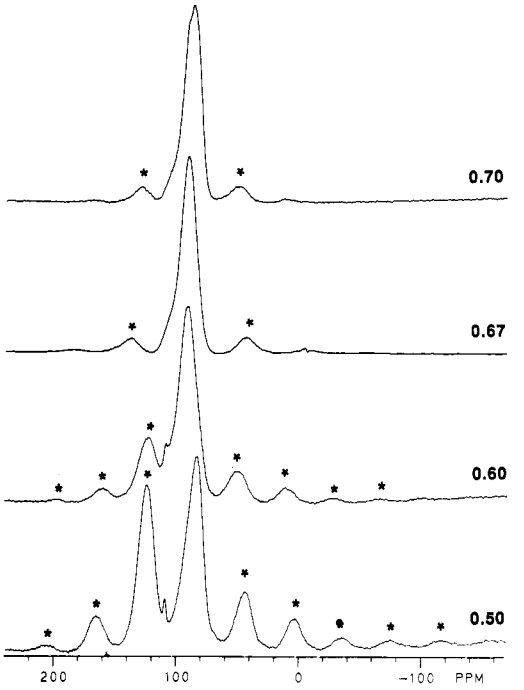

Figure 3. ^{31}P MAS NMR spectra of glasses in the system $(Li_2S)_x$–$(P_2S_5)_{1-x}$. The respective values of x are indicated in the figure. Spinning sidebands are indicated by asterisks.

Table II further indicates that, for a given compound, the ^{6}Li MAS NMR signals are 1 order of magnitude sharper than the corresponding ^{7}Li resonance, resulting in substantially improved resolution (see also Figure 2c). As pointed out previously, this is easily explained on the basis of the different nature of line-broadening mechanisms for these resonances (^{7}Li, homogeneous; ^{6}Li, inhomogeneous).[44]

NMR Characterization of Glasses in the System Li_2S–P_2S_5. Figure 3 shows the compositional dependence of the ^{31}P MAS NMR spectra in binary Li_2S–P_2S_5 glasses. For $x = 0.4$ (not shown) and 0.5, a site with intense spinning sidebands, indicative of a large chemical shift anisotropy is observed. Orientation and magnitude of this anisotropy are consistent with an interpretation in terms of a sulfur analogue of a metaphosphate group, i.e., a polymeric $Q^{(2)}$ species. We note that at both $x = 0.4$ and 0.5, the isotropic chemical shift as well as the anisotropic components are distinctly different between the crystalline and the glassy materials, revealing major structural differences (see further discussion below).

With increasing x, the spinning sideband intensities in Figure 3 decrease dramatically. This observation is entirely consistent with the model that, at higher Li_2S contents, the $Q^{(2)}$ chain units are successively replaced by dimeric $Q^{(1)}$ and monomeric $Q^{(0)}$ units. As is well-documented in the literature for phosphorus–oxygen compounds,[38] the $Q^{(1)}$ and $Q^{(0)}$ species, as a result of their higher symmetry, generally have chemical shift anisotropies that are substantially smaller than those of $Q^{(2)}$ species, hence giving rise to weaker spinning sidebands. At $x = 0.66$, the spectra show a dominant peak centered near 90 ppm. Again, this shift is distinctly different from that in the crystalline counterpart, $Li_4P_2S_6$. On the basis of the composition, we assign this peak to dimeric $Q^{(1)}$ (pyrothiophosphate, $P_2S_7^{4-}$) groups. This assignment is supported further by the ^{31}P chemical shift of $Ag_4P_2S_7$ (the only crystallographically well-characterized related compound containing the $P_2S_7^{4-}$ entity), measured to be 96.6 ppm vs H_3PO_4. The ^{31}P MAS NMR spectrum of the glass with the intermediate com-

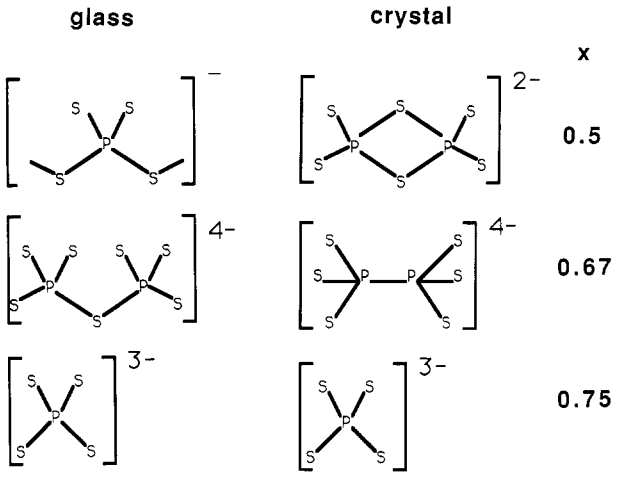

Figure 4. Proposed structural units occurring in crystalline and glassy compositions of the system $(Li_2S)_x(P_2S_5)_{1-x}$. The respective values of x are indicated in the figure.

position of $x = 0.6$ can be simulated quantitatively as a superposition of approximately equal amounts of $Q^{(1)}$ and $Q^{(2)}$ species, as expected on the basis of the composition of this glass. The spectrum of the glass with $x = 0.7$ shows a MAS centerband that appears to be multicomponent. While the quantitative simulation is more ambiguous in this case, the splitting is explained qualitatively by assuming that (as expected) $P_2S_7^{4-}$ and PS_4^{3-} groups coexist at this stoichiometry. Finally, all of the spectra show, reproducibly, a minority peak (shoulder containing ca. 10% of the total signal area) at 103–105 ppm. On the basis of the results obtained on $Li_4P_2S_6$, we assign this resonance to species with the P–P-bonded hexathiohypodiphosphate environment, having formed by sulfur loss. The NMR spectra reveal that this process, which is complete in the crystalline state, appears to be of only minor importance in the glasses.

The ^6Li MAS NMR spectra of the glasses show single sharp (20–30 Hz wide) lines with a monotonic increase of δ_{iso} as x is increased. Generally, these results are in accordance with those obtained on other chalcogenide glass systems.[44,45,47]

Discussion

Structural Aspects of the Glass-to-Crystal Transition in the System Li_2S–P_2S_5. Figure 4 juxtaposes the proposed microenvironments present in glasses and crystalline compounds of the system Li_2S–P_2S_5 as a function of composition. One remarkable feature of this system is the apparent instability of the $P_2S_7^{4-}$ ($Q^{(1)}$) group in the crystalline state with respect to disproportionation into $P_2S_6^{4-}$ and elemental sulfur at *any* composition. Indeed, not many pyrothiophosphates have been well-characterized,[52] in contrast to the large number of crystalline hexathiohypodiphosphates.[57–59] Since the NMR data of the present study indicate that the $P_2S_7^{4-}$ group can be easily preserved in the glassy state, we conclude that the decomposition of this group upon crystallization is essentially driven by a high lattice energy of $Li_4P_2S_6$. The disproportionation reaction of the thiopyrophosphate group provides an example where homoatomic P–P and S–S bonds compete successfully with the formation of the heteroatomic bond. Another well-known example in the P–S system is the crystalline compound P_4S_7, which contains a P–P bond, contrary to the corresponding oxide.[66]

In glasses, the tendency to form homoatomic bonding is generally less pronounced. Specifically, no evidence for homoatomic bonding has ever been found to occur in lithium-based chalcogenide glasses, such as Li_2S–SiS_2 or Li_2S–B_2S_3. In contrast, the NMR results of the present study suggest that in Li_2S–P_2S_5 glasses up to 10% of the phosphorus atoms can occur in a P–P-bonded fashion, giving rise to the shoulder at 103–105 ppm.

In this connection, the possible existence of edge-sharing units in the present glasses has to be discussed. Edge-sharing units, which constitute a violation of the Zachariasen bonding principle,[67] have been previously quantified by ^{29}Si MAS NMR in a variety of non-oxide chalcogenide glasses, including the systems Si–S, Si–Se,[46] and Li_2S–SiS_2.[68] A common theme to all of these studies, however, is that the tendency toward edge-sharing is generally much more pronounced in the crystalline than in the glassy state. This may explain the large chemical shift change upon the glass-to-crystal transition at $x = 0.5$. $LiPS_3$ resonates almost 30 ppm upfield of the glass with identical composition and also has a significantly larger chemical shift anisotropy. The same observation has been made (at $x = 0.5$) in the system Li_2S–SiS_2 and has been attributed conclusively to edge-sharing in the crystalline compound. These edge-sharing units are shifted significantly upfield and have large chemical shift anisotropies compared to the corner-sharing ones. Assuming the same to be true in phosphorus sulfide compounds, we assign the 54.9 ppm signal in crystalline $LiPS_3$ to dimeric $P_2S_6^{2-}$ edge-shared groups. The 83 ppm signal observed in the glasses is then assigned to chain units analogous to the metaphosphate groups found in phosphate glasses. However, compared to Li_2S–SiS_2 glasses, Li_2S–P_2S_5 glasses have a much lower tendency to form edge-shared coordination polyhedra.

Comparison between Phosphorus-Based Sulfide and Oxide Glasses. Overall, the principles governing the structure of Li_2S–P_2S_5 glasses are found to be quite similar to those in alkali-metal phosphate glasses. Addition of lithium sulfide to P_2S_5 introduces nonbridging sulfur atoms, resulting in a continuous network transformation of $Q^{(n)}$ species, as illustrated in Figure 4. These structural changes are conveniently monitored by ^{31}P solid-state NMR, which allows identification and (to a certain extent) quantitation of $Q^{(2)}$, $Q^{(1)}$, and $Q^{(0)}$ units. Contrary to phosphate glasses, no $Q^{(3)}$ units are detectable in phosphorus sulfide based glasses. As previously observed in a similar comparison of the systems M_2S–SiS_2 and M_2O–SiO_2 (M = Li, Na), the ^{31}P (and ^{29}Si) chemical shift differences between the various $Q^{(n)}$ species are substantially smaller in the sulfide, compared to the oxide systems.[47,68] While this leads to problems in corresponding peak assignments for thiosilicate glasses,[47] the distinction between the $Q^{(n)}$ species in Li_2S–P_2S_5 glasses is easier, partly because of larger differences in the spinning sideband patterns (arising from the chemical shift anisotropies).

The small differences between the $Q^{(n)}$ species in the sulfide glasses suggest that the negative charge generated on a nonbridging sulfur atom is less localized. This may account for the unusually large mobility of the lithium ions in these glasses.

Conclusions

Solid-state NMR, DSC, and X-ray powder diffraction have been used to elucidate the composition and structural properties of glassy and crystalline phases in the system

(66) Vos, A.; Othof, R.; Van Bolhuis, F.; Botterweg, R. *Acta Crystallogr.* **1965**, *19*, 864.

(67) Zachariasen, W. W. *J. Am. Ceram Soc.* **1932**, *54*, 3841.

(68) Eckert, H.; Kennedy, J. H.; Pradel, A.; Ribes, M. *J. Noncryst. Solids* **1989**, *113*, 287.

Li_2S–P_2S_5. The compositional dependence of the NMR and X-ray data consistently indicates the existence of four pseudobinary crystalline compounds with the stoichiometries $LiPS_3$, $Li_4P_2S_6$, Li_3PS_4, and Li_7PS_6, whose structural environments have been characterized by anisotropic solid-state NMR chemical shielding parameters. With the exception of Li_3PS_4, the structural arrangements existing in these crystalline compounds have no counterpart in the analogous oxide system Li_2O–P_2O_5.

The results of the present study emphasize the significance of non-oxide chalcogenide glasses from the viewpoint of structural chemistry. Contrary to oxide glasses, which can be viewed as random arrangements of local environments already known in crystalline compounds, chalcogenide glasses show local environments unique to the glassy state that appear unstable in the crystalline form. Overall, the glassy state tends to favor connectivities more analogous to those present in oxidic glasses; i.e., corner-sharing is favored over edge-sharing and dimeric thiopyrophosphate groups are favored over the hexathiohypodiphosphate units. Current NMR investigations focus on the question of how this distribution of structural units can be influenced by coformers such as Al_2S_3, B_2S_3, and SiS_2. This question is relevant with respect to the role these coformers play in determining the stability of the solid electrolyte against the lithium anode materials in battery cells.[69,70]

Acknowledgment is made to the donors of the Petroleum Research Fund, administered by the American Chemical Society, and to the UCSB Academic Senate for financial support of this research.

Registry No. Li_2S, 12136-58-2; P_2S_5, 1314-80-3; Li, 7439-93-2; P, 7723-14-0; S, 7704-34-9; $LiPS_3$, 126901-01-7; $Li_4P_2S_6$, 82866-99-7; Li_3PS_4, 82857-67-8; Li_7PS_6, 62047-15-8.

(69) Kennedy, J. H.; Zhang, Z. *Solid State Ionics* **1988** *28–30*, 726.
(70) Kennedy, J. H.; Zhang, Z. *J. Electrochem. Soc.* **1989**, *136*, 2441.

Electron Microscopy Study of Delamination in Dispersions of the Perovskite-Related Layered Phases $K[Ca_2Na_{n-3}Nb_nO_{3n+1}]$: Evidence for Single-Layer Formation

M. M. J. Treacy,* S. B. Rice, A. J. Jacobson,* and J. T. Lewandowski

Exxon Research and Engineering Company, Annandale, New Jersey 08801

Received November 27, 1989

Intercalation of basic surfactant molecules into the layered perovskites $H[Ca_2Na_{n-3}Nb_nO_{3n+1}]$, n = 3–5, can be used to cause spontaneous exfoliation of the structure into thin sheets that form stable dispersions in a polar solvent. The extent of exfoliation has been determined by examining Rutherford scattered intensities into a high-angle annular dark-field detector in a scanning transmission electron microscope. It is shown that for $n \leq 5$, the layered perovskites can be exfoliated to form single layers. Exfoliation is easiest for the n = 3 and 4 materials.

Introduction

A series of compounds, $A[Ca_2Na_{n-3}Nb_nO_{3n+1}]$ (A = K, Rb, Cs), n = 3–7,[1-4] has recently been shown to have perovskite-related layered structures, as illustrated schematically in Figure 1 for the potassium compound with n = 3. The detailed structure has been determined for one of the end members, $Cs[Ca_2Na_{n-3}Nb_nO_{3n+1}]$, n = 3.[2] The structure comprises perovskite-like layers of NbO_6 octahedra that are terminated along one of the perovskite cubic directions. The layers are n octahedra thick and contain n – 1 cations that are all calcium atoms when n = 3 or disordered sodium and calcium atoms when n > 3. Other related compounds, $KLnNb_2O_7$ (Ln = La, Nd),[4,5] $A_2Ln_2Ti_3O_{10}$ (A = Na, K, Rb and Ln = La, Nd, Sm, Gd, Dy),[6,7] and $ABiNb_2O_7$ and $APb_2Nb_3O_{10}$ (A = Rb, Cs)[8] have recently been described. An unusual feature of all of these phases is that they readily ion exchange the interlayer cations. Exchange has been observed in molten salts[1] and by treatment in aqueous acid at ambient to slightly elevated temperatures.[1,3-9] In the latter case, the compounds formed, for example, the $H[Ca_2Na_{n-3}Nb_nO_{3n+1}]$ series, are solid acids and can react further with organic bases to form intercalation compounds with large interlayer expansions.[10] Insertion of long-chain organic amines between the perovskite layers produces a large volume expansion, and individual crystallites begin to exfoliate to form sheets that are very thin in the direction perpendicular to the layers. A scanning electron micrograph (Figure 2) of a crystal of $H[Ca_2Nb_3O_{10}]$ that has been intercalated with octadecylamine shows the beginning stages of layer separation. The limiting case of this process is the complete breakdown of the crystal into single layers. The phenomenon is known to occur in several systems, particularly in the smectite clay minerals, which are well known to spontaneously exfoliate in water.[11] Other systems with comparable layer charges behave similarly, e.g., Na_xMS_2,[12-14] FeOCl,[15] and

(1) Dion, M.; Ganne, M.; Tournoux, M. *Mater. Res. Bull.* **1981**, *16*, 1429–1435.
(2) Dion, M.; Ganne, M.; Tournoux, M. *Rev. Chim. Mineral.* **1984**, *21*, 92–103.
(3) Jacobson, A. J.; Johnson, J. W.; Lewandowski, J. T. *Inorg. Chem.* **1985**, 3727–3729.
(4) Dion, M.; Ganne, M.; Tournoux, M. *Rev. Chim. Mineral.* **1986**, *23*, 61–69.
(5) Gopalakrishnan, J.; Bhat, V.; Raveau, B. *Mater. Res. Bull.* **1987**, *22*, 413–417.
(6) Gondrand, M.; Joubert, J.-C. *Rev. Chim. Mineral.* **1987**, *24*, 33–41.
(7) Gopalakrishnan, J.; Bhat, V. *Inorg. Chem.* **1987**, *26*, 4299–4301.
(8) Subramanian, M. A.; Gopalakrishnan, J.; Sleight, A. W. *Mater. Res. Bull.* **1988**, *23*, 837–842.
(9) Jacobson, A. J.; Lewandowski, J. T.; Johnson, J. W. *J. Less Common Met.* **1986**, *116*, 137–146.
(10) Jacobson, A. J.; Johnson, J. W.; Lewandowski, J. T. *Mater. Res. Bull.* **1987**, *22*, 45–51.
(11) Grim. R. E. *Clay Mineralogy*, 2nd ed.; McGraw-Hill: New York, 1968.
(12) Lerf, A.; Schollhorn, R. *Inorg. Chem.* **1977**, *16*, 2950–2956.
(13) Murphy, D. W.; Hull, Jr., G. W. *J. Chem. Phys.* **1975**, *62*, 973–978.

0897-4756/90/2802-0279$02.50/0